JOURNAL OF THEORETICAL AND APPLIED MECHANICS
51, 2, pp. 349-362, Warsaw 2013

EXTENSION OF THE CONCEPT OF LIMIT LOADS FOR 3D CASES FOR A CENTRALLY CRACKED PLATE IN TENSION

Marcin Graba
Kielce University of Technology, Faculty of Mechatronics and Machine Design, Kielce, Poland
e-mail: mgraba@tu.kielce.pl

In the paper, the verification of the limit load solutions for a centrally cracked plate under tension (CC(T)) is presented using FEM calculations. Numerical calculations and analysis of the obtained FEM results were used to recalculation of the existing limit load formulas proposed by EPRI procedures for plane strain and plane stress. After verification of the EPRI solutions, three dimensional FEM calculation was done to determine the limit loads for 3D cases of CC(T) specimens. The measurable effect of the paper is a catalogue of numerical solutions and their approximations, which may be useful in the engineering analysis.

Key words: fracture mechanics, cracks, FEM, limits loads, load-line displacement, CC(T) specimen

1. Introduction and basis for the engineering approach (based on Kumar *et al.* (1981))

In the literature, three recent developments in the elastic-plastic fracture mechanics have made the development of an engineering approach practical. The first of these is the identification of J-integral or Crack Opening Displacement (COD) as suitably characterizing parameters for ductile fracture, and the development of the resistance curve approach based on these parameters for crack growth predictions. The second of these is the development of an elastic-plastic estimation procedure for cracked bodies, which were presented by Kumar *et al.* (1981) in EPRI procedure. And the third of these is the development of an incompressible finite element suitable for fully plastic calculations. The use of the J-integral (Rice, 1968a,b) for characterizing crack initiation in ductile materials under large-scale yielding conditions was proposed by Begley and Landes (1972). The suggestion that a relationship exists between the J-integral and the amount of stable crack growth was made in studies by Rice *et al.* (1973), Paris *et al.* (1979), Hutchinson and Paris (1979) and Shih *et al.* (1981).

The elastic-plastic estimation procedure is derived from the work by Shih (1976), Shih and Hutchinson (1976), Bucci *et al.* (1972) and Rice *et al.* (1973). The presented by Kumar *et al.* (1981) procedure was based on a quite simple idea. The idea is to estimate the elastic-plastic solutions by interpolating in a suitable fashion between the fully plastic solutions and the elastic solutions.

The characterization of stress and strain fields near the crack tip by the J-integral is analogous to the use of the stress intensity factor K as the characterizing parameter in the linear elastic fracture mechanics. The papers presented by Hutchinson (1968) and Rice and Rosengren (1968) revealed that, for stationary cracks, the stresses in the vicinity of the crack tip under yielding conditions varying from small-scale to fully plastic may be represented by following formulas

$$\sigma_{ij} = \sigma_0 \Big(\frac{J}{\alpha \sigma_0 \varepsilon_0 I_n r} \Big)^{\frac{1}{1+n}} \widetilde{\sigma}_{ij}(\theta, n) \tag{1.1}$$

where r and θ are polar coordinates of the coordinate system located at the crack tip, σ_{ij} are components of the stress tensor, J is the J-integral, n is R-O exponent, α is R-O constant, σ_0 is yield stress, ε_0 is strain related to σ_0 through $\varepsilon_0 = \sigma_0/E$. Functions $\widetilde{\sigma}_{ij}(n,\theta)$, $I_n(n)$ must be found by solving the fourth order non-linear homogenous differential equation independently for the plane stress and plane strain (Hutchinson, 1968). The full algorithm and the computer program for evaluation of these functions are presented in Gałkiewicz and Graba (2006). Equation (1.1) is commonly called the "HRR solution".

The crack tip field equations (see Eq. (1.1)) can also be expressed in terms of the crack tip opening displacement. If the crack tip opening displacement denoted as δ_T is defined as the opening distance where 45° lines intercept the crack faces, the J-integral and crack tip opening displacement δ_T are linked by the following relationship

$$\delta_T = d_n \frac{J}{\sigma_0} \tag{1.2}$$

where d_n is a tabulated function of σ_0/E work hardening exponent, and takes different values for plane strain and plane stress (Shih, 1981). This function can be determined using the computer program presented by Gałkiewicz and Graba (2006).

When the HRR field encompasses the fracture process zone, the parameters J-integral and crack tip opening displacement are natural candidates to characterize fracture (Kumar *et al.*, 1981).

2. Engineering approach to the fracture mechanics – fully plastic solutions (based on Kumar *et al.* (1981))

As indicated earlier (what was presented by Kumar *et al.* (1981), and (R5, 1998), (R6, 2001), the key to develop the engineering approach rests in the ability to tabulate fully plastic crack solutions for a broad range of representative structural configurations. Such tabulations are of course already available for linear elasticity (Rooke and Cartwright, 1976; Tada *et al.*, 1973).

In linear elasticity (Kumar *et al.*, 1981), the crack parameters like the J-integral, the crack or mouth opening displacement δ and the load line displacement Δ_c (due to crack) can be scaled with respect to load according to the following relationships

$$\frac{J}{\sigma_0 \varepsilon_0 a} = \Big(\frac{P}{P_0}\Big)^2 \hat{J}^e\Big(\frac{a}{W}\Big) \qquad \frac{\delta}{\varepsilon_0 a} = \frac{P}{P_0}\hat{\delta}^e\Big(\frac{a}{W}\Big) \qquad \frac{\Delta_c}{\varepsilon_0 a} = \frac{P}{P_0}\widehat{\Delta}_c^e\Big(\frac{a}{W}\Big) \tag{2.1}$$

where the superscript e denotes elastic quantities. In Eqs. (2.1), P is a generalized load per unit thickness, a/W is crack length to width ratio, σ_0 is yield stress, reference stress or, in some applications, the flow stress, and ε_0 is the corresponding strain (the connection $\sigma_0 = E\varepsilon_0$ can always be made, but is not necessary). The quantities J, δ and Δ_c are functions of a/W only. P_0 is the limit or reference load per unit thickness based on the stress σ_0, defined as

$$P_0 = \Lambda b \sigma_0 \tag{2.2}$$

where Λ is the constraint factor which may depend on the ratios of relevant structure dimensions, and b is the length of the uncracked ligament. The EPRI procedure (Kumar *et al.*, 1981) presents the limit loads formula only for the plane stress and plane strain separately.

Based on the HRR solution (Hutchinson, 1968; Rice and Rosengren, 1968), the analysis presented by Ilyushin (1946) and considerations presented by Kumar *et al.* (1981), for a fully plastic material, it can be noted that the simple functional dependence of the field quantities on the applied load or displacement also means that quantities such as the J-integral, the crack

opening displacement δ and other crack parameters have the following forms (Goldman and Hutchinson, 1975)

$$\frac{J}{\alpha\sigma_0\varepsilon_0 a} = \Big(\frac{P}{P_0}\Big)^{n+1}\hat{J}^p\Big(\frac{a}{W},n\Big) \qquad \frac{\delta}{\alpha\varepsilon_0 a} = \Big(\frac{P}{P_0}\Big)^{n}\hat{\delta}^p\Big(\frac{a}{W},n\Big)$$
$$\frac{\Delta_c}{\alpha\varepsilon_0 a} = \Big(\frac{P}{P_0}\Big)^{n}\widehat{\Delta}_c^p\Big(\frac{a}{W},n\Big) \tag{2.3}$$

where the applied load appears explicitly in the manner shown, and the superscript p denotes fully plastic quantities. The dimensionless quantities $\hat{J}^p$, $\hat{\delta}^p$ and $\widehat{\Delta}_c^p$ are functions of only a/W and n and are independent of the applied load (Kumar *et al.*, 1981).

If the presented solution is to be used for elastic-plastic analysis, appropriate Eqs. (2.1) and (2.3) must be added (Kumar *et al.*, 1981). It can be noted, as presented by Kumar *et al.* (1981), the elastic, fully plastic or elastic-plastic estimation procedure requires knowledge of the limit load P_0, which was presented by Eq. (2.2). In 1981, Kumar *et al.* (1981) presented some fully plastic solutions and limit load equations for a centrally cracked plate – CC(T) for a compact specimen – C(T), for a single edge notch specimen in bending – SEN(B) or in tension – SEN(T), and for a double edge notch specimen in tension – DEN(T). All these elements were used to idealize the complex structural components, what was presented in (SINTAP, 1999; FITNET, 2006).

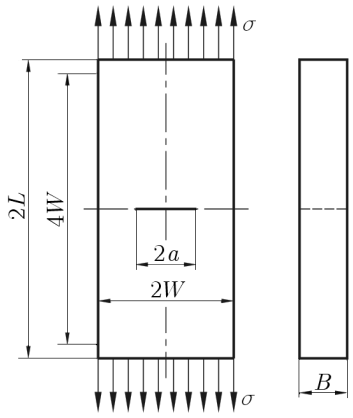

Fig. 1. Centrally cracked plate in tension (CC(T) specimen)

The geometry under consideration is often a centrally cracked plate in tension (CC(T) specimen) – see Fig. 1. This geometry was used to determine the relationship between J-integral and Q-stress defined by O'Dowd and Shih (1991, 1992), what was discussed by Graba (2012). The CC(T) geometry was used by Sumpter and Forbes (1992) to determine the fracture toughness in low temperature. This geometry was also used by Neimitz *et al.* (2004) to assess the fracture toughness and fracture mechanism of construction steels. The presented by Kumar *et al.* (1981) limit load analysis of this configuration leads to the following relationships for determination of the limit load

$$P_0 = \begin{cases} 2b\sigma_0 & \text{for plane stress} \\ \dfrac{4}{\sqrt{3}}b\sigma_0 & \text{for plane strain} \end{cases} \tag{2.4}$$

where b is the uncracked ligament of the specimen, $b = W - a$.

As we can see, this solution is only true for plane stress or plane strain. It can be noted that this approach does not take into account the effect of thickness of the structural component. If an engineer needs the limit load for a three-dimensional case, he uses a model for the plane stress

assuming a unit thickness, and then multiplies the result by the corresponding thickness reference value. Such behavior leads to achievement of a conservative result which may be different from the real external load of the structural component.

Thus, the above presented relationships for plane stress and plane strain will be verified numerically by using the Finite Element Method (FEM), and then three dimensional calculations will be done based on the newly proposed formulas for finding the limit loads, which take into consideration the specimen thickness, not included in Eqs. (2.4). A similar verification of the limits load solutions for plane stress and plane strain for single edge notched specimen (SEN(T)) was presented in 2013 (Graba, 2013).

3. Details of the numerical analysis to verify the EPRI solutions for plane stress and plane strain – 2D cases

In the numerical analysis, the centrally cracked plate in tension (CC(T)) was used (Fig. 1). Dimensions of the specimens satisfy the standard requirement which is set up in FEM calculation $L \geqslant 2W$, where W is the width of the specimen and L is the measuring length of the specimen. Computations were performed for the plane strain and plane stress using a small strain option. The relative crack length was $a/W = \{0.05, 0.20, 0.50, 0.70\}$ where a is the crack length, and the width of specimens W was equal to 40 mm (in this case, the measuring length $L \geqslant 80$ mm). All geometrical dimensions of the CC(T) specimen are presented in Table 1.

Table 1. Geometrical dimensions of the CC(T) specimen used in numerical analysis

Width W [mm]	Measuring length $4W$ [mm]	Total length $2L$ [mm]	Relative crack length a/W	Crack length a [mm]	AA $b = W - a$ [mm]
40	160	176	0.05	2	38
			0.20	8	32
			0.50	20	20
			0.70	28	12

AA – length of the non-cracked section of the specimen

The choice of the CC(T) specimen was intentional, because CC(T) specimens are used in the FITNET procedures (FITNET, 2006) to model real structural elements. Also in FITNET procedures (FITNET, 2006), the limit load and stress intensity factors solutions for CC(T) specimens are presented. However, in the EPRI procedures (Kumar *et al.*, 1981), the hybrid method for calculation of the J-integral, crack opening displacement (COD) or crack opening displacement (CTOD) is given, but the presented by EPRI (Kumar *et al.*, 1981) limit load solutions are different form the FEM results. Also some laboratory tests in order to determine the critical values of the J-integral may be done using the CC(T) specimen (Neimitz *et al.*, 2004). The ASTM E 1820-05 standard requirements (ASTM 1820-05, 2005) dictate that the plane strain fracture toughness is determined using the SEN(B) specimen – a single edge notch specimen in bending.

Computations were performed using ADINA SYSTEM 8.7.3 (ADINA, 2008a,b). Due to the symmetry, only a quarter of the specimen was modeled. The finite element mesh was filled with the 9-node plane strain or plane stress elements. The size of the finite elements in the radial direction was decreasing towards the crack tip, while in the angular direction the size of each element was kept constant. The crack tip region was modeled using 36-50 semicircles. The first of them, was at least 20 times smaller than the last one. It also means that the first finite element behind the crack tip is smaller 2000 times than the width of the specimen. The crack

tip was modeled as a quarter of the arc whose radius was equal to $r_w = 1 \cdot 10^{-6}$-$2.5 \cdot 10^{-6}$ m ($2.5 \cdot 10^{-5}$-$6.25 \cdot 10^{-5}$)W). The whole CC(T) specimen was modeled using 323 finite elements and 1353 nodes. The external load was applied to the bottom edge of the specimen. For the plane strain condition in the numerical analysis, the assumed thickness was equal to $B = 1$ m and for the plane stress $B = 1$ mm. The presented numerical model was built according to the literature, given by Brocks *et al.* (2003), Brocks and Scheider (2003) and by Graba and Gałkiewicz (2007).

In the FEM simulation, the model of an elastic-perfectly plastic material was used to calculate the limit load. The analysis was performed for four materials which were differed by the yield stress. In all calculations, the same values of Young's modulus and Poisson's ratio were assumed. The tensile properties for the elastic-perfectly plastic materials, which were used in the numerical analysis, are presented below in Table 2.

Table 2. Mechanical properties of the materials used in numerical analysis (σ_0 – yield stress, E – Young's modulus, ν – Poisson's ratio, ε_0 – strain corresponding the yield stress)

σ_0 [MPa]	E [MPa]	ν	$\varepsilon_0 = \sigma_0/E$
315	206000	0.3	0.00153
500			0.00243
1000			0.00485
1500			0.00728

In the numerical analysis, 32 CC(T) specimens were used which were differed by the crack length (different a/W), yield stress and dominations of the plane stress or plane strain.

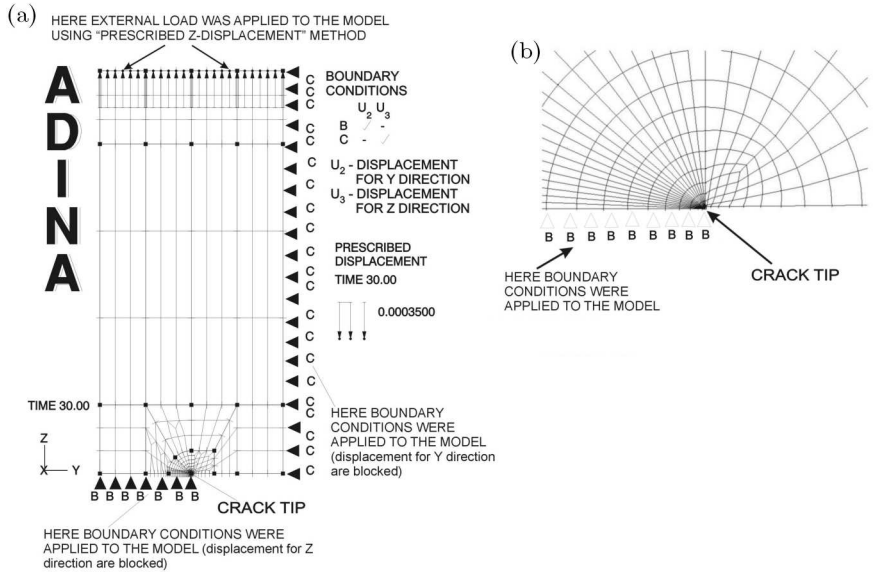

Fig. 2. (a) The finite element model for the CC(T) specimen used in the numerical analysis for 2D cases; (b) the finite elements mesh near the crack tip using in the numerical analysis (2D cases)

4. Results of the numerical analysis for 2D cases and comparison with the EPRI solutions

Evaluation of the achievements by the CC(T) specimen of full plasticity, and thereby with the state of the load limit achieved, were performed on the basis of the evolving plastic zone near the crack tip and a graph of the external force P as a function of the load line displacement v_{LL}. For all the analyzed specimens, graphs presenting the external load as a function of the load line

displacement were made. Analysis of each graph was done with simultaneous evaluation of the plastic zone. For the limit load the value of the external load is considered, which is read from a graph of the external load P as a function of the load line displacement v_{LL}, from the horizontal segment of the $P = f(v_{LL})$ curve (plateau on the graph $P = f(v_{LL})$), which corresponds to full plasticity of the uncracked ligament of the specimen.

In Fig. 3, some graphs obtained in the numerical analysis of the external load as a function of the load line displacement are presented. Based on these charts and schedules of the plastic zone for each analyzed specimen, the limit load value was determined as a constant value of the external load from the graph. The results of this analysis are presented in Table 3.

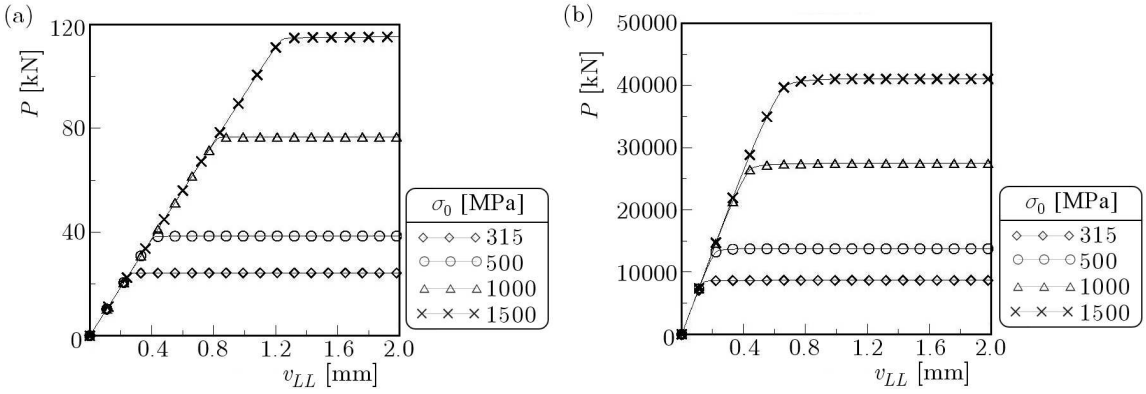

Fig. 3. Graphs of the external load P changes as a function of the load line displacement v_{LL} for CC(T) specimens ($E = 206\,\text{GPa}$, $\nu = 0.3$, $W = 40\,\text{mm}$: (a) $a/W = 0.05$, dominated by plane stress – specimen thickness in the numerical analysis was equal to $B = 1\,\text{mm}$; (b) $a/W = 0.70$, dominated by plane strain – specimen thickness in the numerical analysis was equal to $B = 1\,\text{m}$

Table 3. Estimated numerically limit load values for CC(T) specimens for plane stress and plane strain

σ_0 [MPa]	Plane stress ($B = 1\,\text{mm}$)				Plane strain ($B = 1\,\text{m}$)			
	a/W				a/W			
	0.05	0.20	0.50	0.70	0.05	0.20	0.50	0.70
	P_0 [kN]				P_0 [kN]			
315	24.23	20.22	12.54	7.47	28037.56	23377.87	14503.78	8664.88
500	38.45	32.09	19.90	11.85	44467.61	37086.82	23016.53	13750.97
1000	76.69	64.08	39.75	23.70	88108.58	73861.20	45931.68	27476.47
1500	115.22	96.21	59.67	35.48	133125.62	111126.04	69000.41	41061.70

In Fig. 4, the influence of the relative crack length and yield stress on the limit load are presented. Analysis of the obtained numerical results indicates a few obvious, almost natural conclusions:

- limit load values for the plane strain cases are greater than for plane stress cases, if the same value of the specimen thickness is a reference value;
- for higher values of the yield stress, greater values of the limit load are observed;
- an increase in the crack length causes a decrease in the value of the limit load.

Analysis of the obtained numerical results indicates a proportional limit load dependence of the yield stress and crack length, what may be observed in Fig. 4.

In Fig. 5, a comparison of the plastic zones for plane stress and plane strain was presented for the normalized external load $P/P_0 = 1.00$. It can be noted that for the same value of the

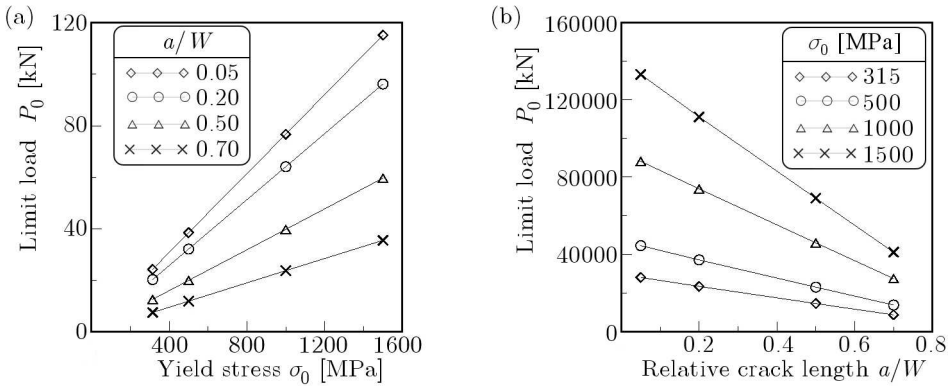

Fig. 4. (a) Influence of the relative crack length a/W on the limit load P_0 for CC(T) specimens ($E = 206\,\text{GPa}$, $\nu = 0.30$, $W = 40\,\text{mm}$) dominated by plane stress ($B = 1\,\text{mm}$); (b) influence of the yield stress σ_0 on the limit load P_0 for CC(T) specimens ($E = 206\,\text{GPa}$, $\nu = 0.30$, $W = 40\,\text{mm}$) dominated by plane strain ($B = 1m$)

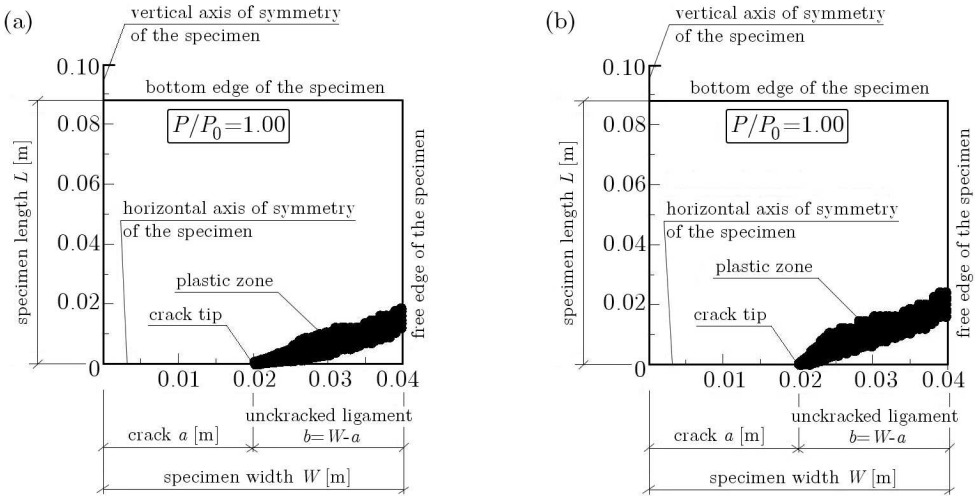

Fig. 5. Comparison of plastic zones for plane stress and plane strain for CC(T) specimen characterized by $a/W = 0.5$, $W = 40\,\text{mm}$, $\sigma_0 = 315\,\text{MPa}$, $E = 206\,\text{GPa}$, $\nu = 0.3$: (a) $P/P_0 = 1.00$, plane stress; (b) $P/P_0 = 1.00$, plane strain

Table 4. Limit loads for CC(T) specimens determined for plane stress and plane strain, using EPRI solutions (Kumar *et al.*, 1981)

σ_0 [MPa]	Plane stress ($B = 1\,\text{mm}$)				Plane strain ($B = 1\,\text{m}$)			
	a/W				a/W			
	0.05	0.20	0.50	0.70	0.05	0.20	0.50	0.70
	P_0 [kN]				P_0 [kN]			
315	23.94	20.16	12.60	7.56	27643.53	23278.76	14549.23	8729.54
500	38.00	32.00	20.00	12.00	43878.62	36950.42	23094.01	13856.41
1000	76.00	64.00	40.00	24.00	87757.24	73900.83	46188.02	27712.81
1500	114.00	96.00	60.00	36.00	131635.90	110851.30	69282.03	41569.22

external load normalized by the appropriate limit load, a larger plastic zone is observed for the plane stress condition for the elastic-perfectly plastic material. Different plastic zones are characterized for the plane stress and plane strain.

All obtained numerical results of the limit loads were compared with the values determined by using Eqs. (2.4) for the plane stress and plane strain respectively (Kumar *et al.*, 1981). Table 4

presents the limit loads which were calculated using the EPRI solutions (Kumar *et al.*, 1981). In Table 5, differences between the numerical solutions and EPRI results (Kumar *et al.*, 1981) are presented, which were calculated as $[(P_{0\_EPRI} - P_{0\_FEM})/P_{0\_EPRI}] \cdot 100\%$, where P_{0_EPRI} is the limit load found from Eqs. (2.4) (for the plane stress or plane strain respectively), and P_{0_FEM} is the limit load value determined by the Finite Element Method (FEM).

Table 5. Difference between EPRI solutions (Kumar *et al.*, 1981) and numerical results of the limit loads for CC(T) specimens for plane stress and plane strain

σ_0 [MPa]	Plane stress ($B = 1\,\text{mm}$)				Plane strain ($B = 1\,\text{m}$)			
	a/W				a/W			
	0.05	0.20	0.50	0.70	0.05	0.20	0.50	0.70
	$[(P_{0\_EPRI} - P_{0\_FEM})/P_{0\_EPRI}] \cdot 100\%$				$[(P_{0\_EPRI} - P_{0\_FEM})/P_{0\_EPRI}] \cdot 100\%$			
315	1.21%	0.30%	0.48%	1.19%	1.43%	0.43%	0.31%	0.74%
500	1.18%	0.28%	0.50%	1.25%	1.34%	0.37%	0.34%	0.76%
1000	0.91%	0.12%	0.63%	1.25%	0.40%	0.05%	0.55%	0.85%
1500	1.07%	0.22%	0.55%	1.44%	1.13%	0.25%	0.41%	1.22%

As one can see, the presented above numerical results agree with the values determined using Eqs. (2.4). The average error between the numerical results and values determined using the EPRI (Kumar*et al.*, 1981) solution is equal to 0.79% for the plane stress and 0.66% for the plane strain.

5. Extension of the concept of limit loads to 3D cases

The presented in EPRI procedures (Kumar *et al.*, 1981) Eqs. (2.4), which may be used to calculate the limit loads, are given for the plane stress or plane strain only. The above presented equations do not include the specimen thickness. In fact, it is rare that a structural element was purely dominated by the plane stress or plane strain. Currently, in the engineering analysis, one of the two formulas is used (valid for plane stress) with including an appropriate value of the specimen thickness. However, the obtained result may actually understate the actual limit load, which the structural component can carry on. Therefore, in this paper, an extension of the limit load patterns to three-dimensional cases is presented (in the analysis, the specimen thickness will be included – the 3D analysis). That analysis will be substantial in the following subsections.

5.1. Details of the numerical analysis in 3D cases

In the three dimensional FEM analysis, the same computer program (ADINA, 2008a, 2008b), material properties (Table 2) and dimension of the CC(T) specimens (Table 1) were used for verification of the EPRI solutions (Kumar *et al.*, 1981). The computations were performed for three dimensional geometry using a small strain option. The relative crack length was $a/W = = \{0.05, 0.20, 0.50, 0.70\}$ where a is the crack length, and the width of specimens W was equal to 40 mm. In the analysis, six specimen thicknesses were tested: $B = \{2, 4, 8, 16, 25, 40\}$ mm. The selected range of the thickness specimens ensures the dominance of plane stress or plane strain and the triaxial state of stress and strain near the crack tip.

The computations were performed using ADINA SYSTEM 8.7.3 (ADINA, 2008a, 2008b). Due to the symmetry, only one eight-th part of the specimen was modeled. The finite element mesh was filled with the 8-node three dimensional brick elements. ADINA (ADINA, 2008a, 2008b) recommends using a 8-node bricks finite elements, for the case of tension dominance.

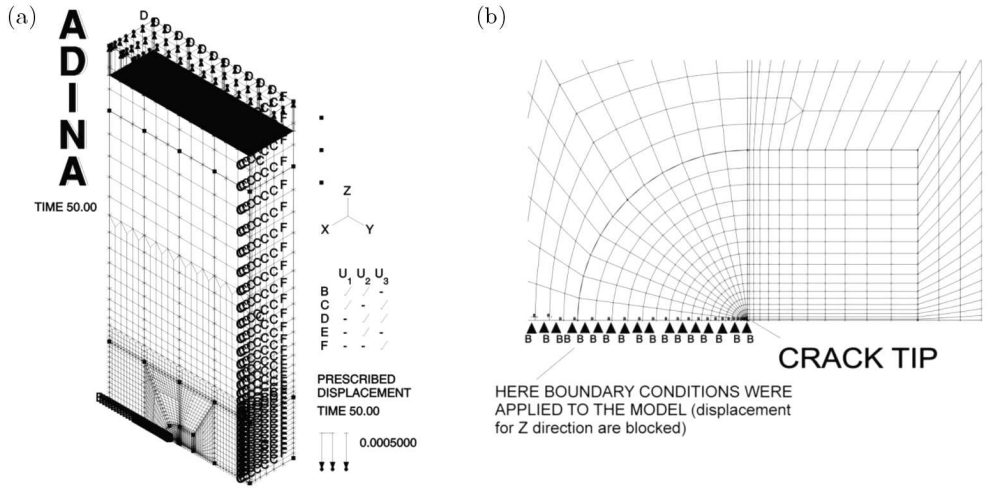

Fig. 6. (a) Finite element model for CC(T) specimen used in numerical analysis for 3D cases; (b) finite elements mesh near the crack tip using in numerical analysis (3D cases)

The size of finite elements in the radial direction was decreasing towards the crack tip, while in the angular direction the size of each element was kept constant. The crack tip region was modeled using 36 semicircles. The first of them was 20 imes smaller than the last one. It also means that the first finite element in front of the crack tip is 2000 times smaller than the width of the specimen. The crack tip is modeled as a quarter of the arc whose radius is equal to $r_w = 1 \cdot 10^{-6}$-$2.5 \cdot 10^{-6}$ m ($2.5 \cdot 10^{-5}$-$6.25 \cdot 10^{-5}$)W). The mesh consists of eight layers of elements (through half the thickness of the SEN(B) specimen). The layer interfaces are located at $x_3/B = \{0, 0.119, 0.222, 0.309, 0.379, 0.434, 0.472, 0.494, 0.5\}$. It should be noted that the layers become thinner as the free surface is approached. The layer in the middle of the specimen is twenty to fifty times thicker than the one near the free surface. The whole CC(T) specimen is modeled using 15552 finite elements and 18018 nodes. An examplary finite element model for the CC(T) specimen for the 3D case is presented in Fig. 5. The presented numerical model was built according to Brocks *et al.* (2003), Brocks and Scheider (2003), Graba and Gałkiewicz (2007) and Graba (2009).

5.2. Numerical results for three dimensional cases

The evaluation of the achievement by the CC(T) specimen of full plasticity, and thereby the state of the load limit, was performed on the basis of the evolving plastic zone near the crack tip and the graph of the external force P as a function of the load line displacement v_{LL}. For all analyzed specimens, graphs presenting the external load as a function of the load line displacement were made. Analysis of each graph was done with simultaneous evaluation of the plastic zone.

For the limit load, the value of the external load is considered, which was read from a graph of the external load P as a function of the load line displacement v_{LL} from the horizontal segment of the $P = f(v_{LL})$ curve (plateau on the graph $P = f(v_{LL})$) corresponding to full plasticity of the uncracked ligament of the specimen.

Figure 7 presents some graphs obtained in the numerical analysis of the external load P as a function of the load line displacement v_{LL}. Based on these and similar charts and schedules of plastic zone for each analyzed specimen, the limit load was determined as a constant value of the external load from the graph. Some results of this analysis are presented in Table 6, which also include a comparison of the numerical results with the values obtained using EPRI procedures (Kumar *et al.*, 1981). In these Tables, the error values were calculated as $E_r = [(P_{0\_EPRI} - P_{0\_FEM})/P_{0\_EPRI}] \cdot 100\%$, where P_{0_FEM} denotes the limit lo-

ad calculated numerically for the 3D specimen and P_{0_EPRI} denotes the limit load calculated using Eqs. (2.4) for the plane stress and plane strain, respectively, using EPRI solutions (Kumar *et al.*, 1981). All the obtained numerical analysis results are available on website: http://www.tu.kielce.pl/∼mgraba/Limits_loads/index.php.

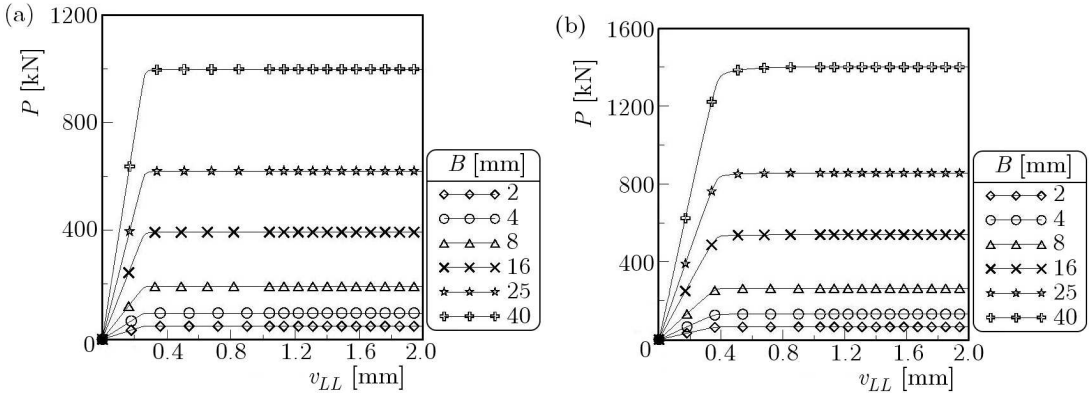

Fig. 7. Graphs of the external load P changes as a function of the load line displacement v_{LL} for CC(T) specimens – 3D cases, $E = 206\,\text{GPa}$, $\nu = 0.30$, $W = 40\,\text{mm}$: (a) $a/W = 0.05$, $\sigma_0 = 315\,\text{MPa}$; (b) $a/W = 0.20$, $\sigma_0 = 500\,\text{MPa}$

Table 6. Selected results of numerical calculations – limit load values for three dimensional CC(T) specimens characterized by different yield stress, crack length and specimen thickness

σ_0 [MPa]	B [m]	a/W	P_0 for 3D case [kN]	P_0 for plane stress EPRI [kN]	P_0 for plane strain EPRI [kN]	E_r for plane stress [%]	E_r for plane strain [%]
315	0.002	0.05	48.60	47.88	55.29	1.48	13.76
315	0.002	0.20	40.93	40.32	46.56	1.49	13.75
500	0.008	0.50	167.20	160.00	184.75	4.31	10.50
500	0.008	0.70	102.31	96.00	110.85	6.17	8.35
1000	0.016	0.05	1259.86	1216.00	1404.12	3.48	11.45
1000	0.016	0.20	1072.56	1024.00	1182.41	4.53	10.24
1500	0.025	0.50	1641.46	1500.00	1732.05	8.62	5.52
1500	0.025	0.70	1006.47	900.00	1039.23	10.58	3.25

In Fig. 8, the influence of yield stress and specimen thickness on the limit loads is presented. Analysis of the obtained numerical results indicates a few obvious, almost natural conclusions:

- limit load values for the specimen characterized by a large thickness are greater than for the specimen characterized by smaller thickness;
- for higher values of the yield stress, greater values of the limit load are observed;
- an increase in the crack length causes a decrease in the value of the limit load.

Analysis of the obtained numerical results indicates a proportional limit load dependence of the yield stress, specimen thickness and crack length, which may be observed in Fig. 8. These two facts will be used in the approximation of the numerical results, which will be discussed in one of the next sections of this paper.

5.3. Approximation of numerical results for 3D cases – new limit loads solution

The presented in the paper and on website http://www.tu.kielce.pl/∼mgraba/Limits_loads/index.php numerical results, from the engineering point of view, can be quite useful when their

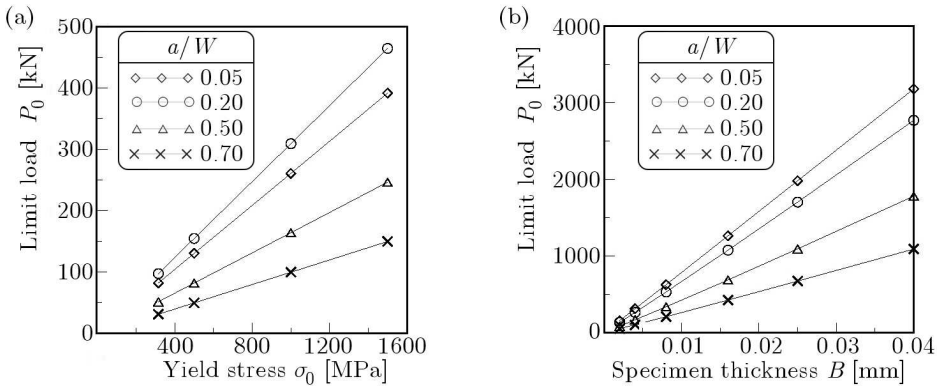

Fig. 8. (a) Influence of the yield stress σ_0 on the limit load P_0 for 3D CC(T) specimens ($E = 206\,\text{GPa}$, $\nu = 0.30$, $W = 40\,\text{mm}$) characterized by $B = 4\,\text{mm}$; (b) influence of the specimen thickness B on the limit load P_0 for 3D CC(T) specimens ($E = 206\,\text{GPa}$, $\nu = 0.30$, $W = 40\,\text{mm}$) characterized by $\sigma_0 = 1000\,\text{MPa}$

use is simple. This can be achieved by implementing the results of numerical approximations. In a general form, the following formula for calculation of the limit load for three-dimensional cases can be proposed

$$P_0 = \sigma_0 f\Big(\frac{a}{W}\Big) \tag{5.1}$$

where $f(B, a/W)$ is a function which depends on the specimen thickness B and relative crack length a/W, which may be expressed by the length of the uncracked ligament of the specimen $b = W - a$. That is why Eq. (5.1) can be written as

$$P_0 = \sigma_0 f(B, b) \tag{5.2}$$

Using the presented in the paper figures and tables, the first stage of the approximation was done. The function $f(B, b)$ for the analyzed geometry may be written as

$$f(B, b) = F_I + F_{II} B^{F_{III}} \tag{5.3}$$

where functions F_I, F_{II}, F_{III} depend on the length of the uncracked ligament of the specimen (relative crack length) $b = W - a = W(1 - a/W)$. The results of the first stage of approximation are presented in Table 7.

Table 7. Coefficients of the approximation in the first stage – Eq. (5.3)

a/W	F_I	F_{II}	F_{III}	R^2
0.05	−0.00276	81.67896	1.007822	0.999995
0.20	0.01060	80.76869	1.046697	0.999946
0.50	0.003705	51.54051	1.045548	0.999989
0.70	−0.00091	30.28136	1.032773	0.999994

In the second stage of the approximation, the numerical results, reciprocal relationship between coefficients F_I, F_{II}, F_{III} and length of the uncracked ligament of the specimen (denoted as $b = W - a$) were found. The results of the second stage of approximation are presented in Table 8.

To take advantage of the presented approximate procedures, the yield stress should be inserted in MPa, and the thickness and the uncracked ligament of the specimen in meters. The obtained result will express the limit load in kN.

Table 8. Numerical results of the second stage of the approximation

a/W	F_I	F_{II}	F_{III}
$\langle 0.05, 0.20\rangle$	$F_I = F_{Ia}b + F_{Ib}$ $R^2 = 1.000$ $F_{Ia} = -2.22645$ $F_{Ib} = 0.08185$	$F_{II} = F_{IIa}b + F_{IIb}$ $R^2 = 1.000$ $F_{IIa} = 151.71$ $F_{IIb} = 75.914$	$F_{III} = F_{IIIa}b + F_{IIIb}$ $R^2 = 1.000$ $F_{IIIa} = -6.47926$ $F_{IIIb} = 1.25403$
$\langle 0.20, 0.70\rangle$	$F_I = F_{Ia}b + F_{Ib}$ $R^2 = 0.999999$ $F_{Ia} = 0.5752763$ $F_{Ib} = -0.0078064$	$F_{II} = \left(F_{IIa} + F_{IIb}\frac{\ln b}{b}\right)^{-1}$ $R^2 = 0.999991$ $F_{IIa} = 0.003844937$ $F_{IIb} = -0.000079388$	$F_{III} = F_{IIIa}[1 - \exp(-F_{IIIb}b)]$ $R^2 = 0.99935$ $F_{IIIa} = 1.0465205$ $F_{IIIb} = 360.9183229$

For different material properties (yield stress σ_0) and different geometrical dimensions (such as the specimen thickness B, relative crack length a/W) which were not included in the numerical analysis, the coefficients F_I, F_{II}, F_{III} and F_{Ia}, F_{Ib}, F_{IIa}, F_{IIb}, F_{IIIa}, F_{IIIb} may be evaluated using the linear or quadratic approximation.

6. Conclusions

In the paper, based on FEM calculations, a verification of the limit load solutions for the CC(T) specimen, which are given in the EPRI procedures (Kumar *et al.*, 1981) was carried out. During calculating the cases of plane strain and plane stress, the limit load values were determined for four elastic-perfectly plastic materials and four relative crack lengths. All numerical results were presented in tabular and graphic forms. Assuming that the FEM model fulfills the requirements presented in the scientific literature (Brocks *et al.*, 2003; Brocks and Scheider, 2003; Graba and Gałkiewicz, 2007; Graba, 2009), the numerically obtained results may be considered as correct. In the next step of the analysis, during three-dimensional FEM analysis, a generalization of these formulas (proposed by EPRI procedures (Kumar *et al.*, 1981)) to three-dimensional cases was done. The proposed new formula of calculation of the limit loads for the CC(T) specimen takes into account the thickness of the structural component (specimen), and yields a less conservative solution than formulas proposed by the EPRI procedures for plane strain or plane stress. For practical applications to solving engineering problems, all the obtained results for the three dimensional cases (which are available on the website) were approximated by mathematical formulas. The integral part of the paper is website http://www.tu.kielce.pl/∼mgraba/Limits_loads/index.php, which presents all the numerical results obtained for three dimensional CC(T) specimens.

The performed numerical calculations and analysis of the obtained results lead to natural conclusions:

- limit load values for the plane strain cases are greater than for the plane stress cases if the same value of the specimen thickness is a reference value;
- for higher values of the yield stress, greater values of the limit load are observed;
- an increase in the crack length causes a decrease in the value of the limit load;
- limit load values for the specimen characterized by a large thickness are greater than for the specimen characterized by a smaller thickness.

In conclusion, it should be noted that the measurable effect of this paper is a catalogue of numerical and analytical solutions for determination of the limit loads for CC(T) specimens for three dimensional cases, which takes into account the effect of the yield stress, crack length and thickness of the structural element.

References

1. ADINA, 2008a, ADINA 8.7.3: ADINA: Theory and Modeling Guide – Volume I: ADINA, Report ARD 08-7, ADINA R&D, Inc., 2008
2. ADINA 2008b, ADINA 8.7.3: ADINA: User Interface Command Reference Manual – Volume I: ADINA Solids & Structures Model Definition, Report ARD 08-6, ADINA R&D, Inc., 2008
3. ASTM E 1820-05 Standard Test Method for Measurement of Fracture Toughness, American Society for Testing and Materials, 2005
4. Begley J.A., Landes J.D., 1972, The J-integral as a fracture criterion in fracture toughness testing, *Fracture Toughness, ASTM Special Technical Publication*, **514**, 1-23, 24-39
5. Brocks W., Cornec A., Scheider I., 2003, Computational aspects of nonlinear fracture mechanics, *Bruchmechanik*, GKSS-Forschungszentrum, Geesthacht, Germany, Elsevier, 127-209
6. Brocks W., Scheider I., 2003, Reliable J-values. Numerical aspects of the path-dependence of the J-integral in incremental plasticity, *Bruchmechanik*, GKSS-Forschungszentrum, Geesthacht, Germany, Elsevier, 127-209
7. Bucci R.J., Paris P.C., Landes J.D., Rice J.R., 1972, J-Integral estimation procedures, *Fracture Toughness, ASTM Special Technical Publication*, **514**, 40-69
8. FITNET Report (European Fitness-for-service Network), Edited by M. Kocak, S. Webster, J.J. Janosch, R.A. Ainsworth, R. Koers, Contract No. G1RT-CT-2001-05071, 2006
9. Gałkiewicz J., Graba M., 2006, Algorithm for determination of $\widetilde{\sigma}_{ij}(n\theta)$, $\widetilde{\varepsilon}_{ij}(n\theta)$, $\widetilde{u}_i(n\theta)$, $d_n(n)$ and $I_n(n)$ functions in Hutchinson-Rice-Rosengren solution and its 3D generalization, *Journal of Theoretical and Applied Mechanics*, **44**, 1, 19-30
10. Goldman N.L., Hutchinson J.W., 1975, Fully plastic crack problems: the center-cracked strip under plane strain, *International Journal of Solids and Structures*, **11**, 575-591
11. Graba M., 2009, Numerical analysis of the mechanical fields near the crack tip in the elastic-plastic materials. 3D problems, PhD dissertation, Kielce University of Technology, Faculty of Mechatronics and Machine Building, p. 387, Kielce [in Polish]
12. Graba M., 2012, The influence of material properties and crack length on the Q-stress value near the crack tip for elastic-plastic materials for centrally cracked plate in tension, *Journal of Theoretical and Applied Mechanics*, **50**, 1, 23-46
13. Graba M., 2013, Numerical verification of the limit load solutions for single edge notch specimen in tension, *Archives of Civil and Mechanical Enginering*, **13**, 1, 45-56
14. Graba M., Gałkiewicz J., 2007, Influence of the crack tip model on results of the finite element method, *Journal of Theoretical and Applied Mechanics*, **45**, 2, 225-237
15. Hutchinson J.W., 1968, Singular behavior at end of tensile crack in hardening material, *Journal of the Mechanics and Physics of Solids*, **16**, 1, 13-31
16. Hutchinson J.W., Paris P.C., 1979, Stability analysis of J-controlled crack growth, *Elastic-Plastic Fracture, ASTM Special Technical Publication*, **668**, 37-64
17. Ilyushin A.A., 1946, The theory of small elastic-plastic deformations, *Prikladnaia Matematika i Mekhanika*, **10**, p. 347
18. Kumar V., German M.D., Shih C.F., 1981 An engineering approach for elastic-plastic fracture analysis, Electric Power Research Institute, Inc. Palo Alto, CA (1981), EPRI Report NP-1931
19. Neimitz A., Dzioba I., Gałkiewicz J., Molasy R., 2004, A study of stable crack growth using experimental methods, finite elements and fractography, *Engineering Fracture Mechanics*, **71**, 1325-1355
20. O'Dowd N.P., Shih C.F., 1991, Family of crack-tip fields characterized by a triaxiality parameter. I Structure of fields, *Journal of the Mechanics and Physics of Solids*, **39**, 8, 989-1015
21. O'Dowd N.P., Shih C.F., 1992, Family of crack-tip fields characterized by a triaxiality parameter. II Fracture applications, *Journal of the Mechanics and Physics of Solids*, **40**, 5, 939-963
22. Paris P.C., Tada H., Zahoor A., Ernst H., 1979, The theory of instability of the tearing mode of elastic-plastic crack growth, *Elastic-Plastic Fracture. ASTM Special Technical Publication*, **668**, 5-36, 251-265

23. R5 – Issue 2, An Assessment Procedure for the High Temperature Response of Structures, British Energy Generation Ltd, 1998
24. R6. Assessment of the Integrity of Structures Containing Defects, Rev. 4. – Gloucester: British Energy Generation Ltd, UK, 2001
25. Rice J.R., 1973, Elastic-plastic models for stable crack growth, *Mechanics and Mechanism of Crack Growth – Proc. at Cambridge, England*, Ed. M.J. May, British Steel Corporation Physical Metallurgy Centre Publication, 1975, 14-39
26. Rice J.R., 1968a, A path independent integral and the approximate analysis of strain concentration by notches and cracks, *Journal of Applied Mechanics*, **35**, 379-386
27. Rice J.R., 1968b, Mathematical analysis in the mechanics of fracture, [In:] *Fracture*, edit. by H. Liebowitz, Vol. II, Academic Press, NY, 191-311
28. Rice J.R., Paris P.C., Merkle J.G., 1973, Some further results on J-integral analysis and estimates, *Progress in Flaw Growth and Fracture Toughness Testing, ASTM Special Technical Publication*, **536**, 231-245
29. Rice J.R., Rosengren G.F., 1968, Plane strain deformation near crack tip in power-law hardening material, *Journal of the Mechanics and Physics of Solids*, **16**, 1, 1-12
30. Rooke D.P., Cartwright J.C., 1976, *Compendium of Stress Intensity Factors*, Her Majesty's Stationary Office, London
31. Shih C.F., 1976, J-Integral estimates for strain hardening materials in antiplane shear using fully plastic solutions, *Mechanics of Crack Growth, ASTM Special Technical Publication*, **590**, 3-22
32. Shih C.F., 1981, Relationships between the J-integral and the crack opening displacement for stationary and extending cracks, *Journal of the Mechanics and Physics of Solids*, **29**, 305-326
33. Shih C.F., de Lorenzi H.G., Andrews W.R., 1979, Studies on crack initiation and stable crack growth, *Elastic-Plastic Fracture, ASTM Special Technical Publication*, **668**, 65-120
34. Shih C.F., Hutchinson J.W., 1976, Fully plastic solutions and large-scale yielding estimates for plane stress crack problems, *Transactions of ASME. Journal of Engineering Materials and Technology. Series H*, **98**, 4, 289-295
35. SINTAP: Structural Integrity Assessment Procedures for European Industry. Final Procedure, Brite-Euram Project No. BE95-1426 – Rotherham: British Steel, 1999
36. Sumpter J.D.G., Forbes A.T., 1992, Constraint based analysis of shallow cracks in mild steel, *TWI/EWI/IS International Conference on Shallow Crack Fracture Mechanics Test and Application*, M.G. Dawes (Ed.), Cambridge, UK, p. 7
37. Tada H., Paris P.C., Irwin G.R., 1973, *The Stress Analysis of Cracks Handbook*, Del Research Corporation, Hellertown, Pennsylvania
38. http://www.tu.kielce.pl/∼mgraba/Limits_loads/index.php

Rozszerzenie koncepcji obciążeń granicznych na przypadki trójwymiarowe dla płyty z centralną szczeliną poddanej rozciąganiu

Streszczenie

W pracy przedstawiono numeryczną weryfikację wzorów pozwalających wyznaczyć obciążenie graniczne dla przypadku płyty z centralną szczeliną poddanej rozciąganiu (próbka CC(T)) dla przypadków płaskiego stanu naprężenia i płaskiego stanu odkształcenia. W kolejnym kroku dokonano rozszerzenia koncepcji wyznaczania obciążeń granicznych na przypadki trójwymiarowe, uwzględniając efekt grubości, wykorzystując szereg trójwymiarowych obliczeń numerycznych. Uzyskane wyniki aproksymowano wzorami analitycznymi. Efektem wymiernym pracy jest katalog rozwiązań numerycznych i ich aproksymacji, pozwalający oszacować obciążenie graniczne dla trójwymiarowego elementu konstrukcyjnego (z uwzględnieniem grubości), bez konieczności prowadzenia czasochłonnych obliczeń numerycznych. Zaprezentowane w pracy wyniki mogą znaleźć zastosowanie w analizie inżynierskiej (np. analiza FAD lub analiza CDF).

Manuscript received April 13, 2012; accepted for print June 21, 2012